

NLOS Detection and Compensation using a Vector Tracking-based GPS Software Receiver

B. Xu, *Interdisciplinary Division of Aeronautical and Aviation Engineering, The Hong Kong Polytechnic University*
L. T. Hsu, *Interdisciplinary Division of Aeronautical and Aviation Engineering, The Hong Kong Polytechnic University*

BIOGRAPHY (IES)

B. Xu is currently a Postdoctoral Fellow with Interdisciplinary Division of Aeronautical and Aviation Engineering, The Hong Kong Polytechnic University. He received his B.S. and Ph.D. degrees in Network Engineering and Navigation Guidance and Control from Nanjing University of Science and Technology, China, in 2012 and 2018, respectively. His research focuses on signal processing in software-defined GNSS receivers.

L. T. Hsu received the B.S. and Ph.D. degrees in aeronautics and astronautics from National Cheng Kung University, Taiwan, in 2007 and 2013, respectively. He is currently an assistant professor with Interdisciplinary Division of Aeronautical and Aviation Engineering, The Hong Kong Polytechnic University, before he served as post-doctoral researcher in Institute of Industrial Science at University of Tokyo, Japan. In 2012, he was a visiting scholar in University College London, U.K. His research interests include GNSS positioning in challenging environment and localization for pedestrian, autonomous driving vehicle and unmanned aerial vehicle.

ABSTRACT

Accurate positioning is highly desirable in urban canyons where satellite signals are easily reflected or blocked by buildings, leading to severe multipath effects or non-line-of-sight (NLOS) receptions. Anti-multipath techniques, e.g., careful antenna or correlator designs, however, have little improvement for NLOS reception. Existing NLOS detection techniques, e.g., the usage of dual-polarization antenna, or fish-eye camera, require external aiding, which is not suitable for low-cost global positioning system (GPS) receivers, e.g., smartphones or wearable devices. In this paper, we use features, such as multi-correlator or code discriminator outputs, extracted at the signal tracking level, to detect NLOS reception in a vector tracking-based software receiver. Multiple correlators with small spacings also help to find the NLOS path delay, which will be further compensated for updating the extended Kalman filter for positioning. Experimental results using real GPS signals in an urban area in Hong Kong show that the proposed method is capable of detecting the NLOS reception and preventing the positioning error from increasing during the NLOS reception period. By comparison, conventional tracking loops would lock onto the incoming NLOS signal and cannot detect its existence, thus reporting an increased positioning error.

INTRODUCTION

Urban canyons, characterized by high-rise buildings or very narrow streets, pose a great challenge for low-cost global positioning system (GPS) receivers, e.g. receivers embedded in smartphones or wearable devices. Satellite signals can easily be blocked or reflected by buildings, leading to multipath effects and none-line-of-sight (NLOS) receptions. In both cases, signals travel an additional distance, adding a bias to the measured pseudorange, which can finally result in a positioning error of several tens of meters [1]. Multipath interference and NLOS reception are, in fact, different effects. Multipath contains both direct and reflected signals, while NLOS contains only the reflected signal. This difference makes the multipath mitigation techniques, e.g. sophisticated antenna designs and careful receiver correlator designs [2, 3], have little improvement for NLOS reception.

A number of approaches to detecting NLOS signals have been proposed in recent years. Based on the fact that direct signals have right-handed circular polarization (RHCP), whereas most reflected signals have left-handed circular polarization (LHCP), a dual-

polarization antenna can be used to distinguish NLOS from direct signals [4]. In [5, 6], a fish-eye camera was used to detect NLOS by first taking pictures of the sky above and then projecting measured satellites onto the image to determine satellite visibility. A similar technology is the usage of 3D light detection and ranging (LiDAR) [7]. In this method, 3D LiDAR is employed to obtain the 3D point cloud of the surrounding environment. Together with the building height information provided by OpenStreetMap (OSM), Skyplot can be generated so that NLOS can be identified. The methods above require additional hardware, which increases the cost, size, weight and power consumption.

In recent years, 3D mapping aided (3DMA) positioning [8] are receiving much attention due to its capability of detecting and mitigating multipath and NLOS effects. With the 3D city model and a candidate user position, a Skyplot with building boundary information can be generated to help predict which signals are blocked [9-11]. Another method aided by 3D city model is the ray-tracing technology, which tracks the signal reflecting routes to identify both multipath and NLOS signals [12]. However, 3DMA GNSS approaches still require the external aiding of 3D map and suffer from the heavy computational load. Thus, methods for detecting NLOS signals that require no hardware nor external aiding should be developed.

Carrier-to-noise ratio (CNR) and elevation angle can both be used as indicators of NLOS reception [13]. However, both features can only partially eliminate NLOS signals, and may also eliminate some direct signals, resulting in less satellite availability or poor satellite geometry. Using consistency checking method to detect NLOS is based on the principle that NLOS measurements would produce a less consistent navigation solution than direct-signal measurements [14, 15]. This method can hardly achieve satisfactory performance when too many inconsistencies exist. These two methods are both applied at the measurement or navigation level. In fact, the measurements of CNR and navigation solution are products of signal tracking. In [16], NLOS reception is detected at the signal processing level, i.e. signal tracking stage. The basic idea is that both multipath and NLOS signals will distort the correlation function of direct signals. Features of NLOS are extracted from the outputs of multiple correlators. An NLOS classifier is then created based on the machine learning of these NLOS features. This method is realized in a conventional tracking-based software receiver, i.e., delay lock loop (DLL) for tracking the code. However, in an NLOS context, the receiver will consider the NLOS signal as a direct signal and keep locking onto it. The maximum correlation value would still be in the prompt channel, which could be hardly used for NLOS detection, especially in the case where only one reflected NLOS signal exists.

An advanced signal tracking technology, vector tracking, has been proven to have the ability of reducing the effects of multipath and NLOS [17, 18], except for its other advantages over conventional tracking, e.g. increased capabilities against weak signal or high dynamic conditions [19, 20]. Unlike conventional tracking, vector tracking predicts the code frequency using not only the measurements but also the propagations of the receiver dynamic model. Therefore, the code tracking loop would not lock onto the incoming code. In other words, the local code replica would be aligned with the “direct” signal (in fact it doesn’t exist), which means there would be a phase difference between the local code and the incoming one, and this difference would manifest itself as a tracking error. Therefore, vector tracking can detect NLOS reception according to the code discriminator or correlator outputs. In particular, multi-correlator also provides an opportunity for detecting the path delay of NLOS signals, which frequently occurs in urban areas. Recently, an open-source vector tracking code based on Matlab is provided [21]. Based on this benefit, this paper proposes to detect the NLOS signals at the signal tracking level using a vector tracking-based GPS software receiver with multiple correlators, and without any other additional aiding. Once detected, the time delay of the NLOS signal would be extracted and compensated to be used in positioning.

In the following sections, the vector tracking design is first introduced, followed by the proposed NLOS reception detection and compensation algorithm. Then, this paper evaluates the performance of the proposed method using real NLOS reception, where the comparison between conventional and vector tracking in terms of NLOS detection is also given. Finally, conclusions are drawn for the paper.

VECTOR TRACKING DESIGN

This section describes the design of the vector delay lock loop (VDLL), including its architecture and the extended Kalman filter (EKF) implementation used in this paper.

Architecture of Vector Tracking

In conventional GPS receivers, each acquired satellite is allocated to an individual tracking channel. Each channel has two closed loops, one for code and one for carrier. The VT-based receiver is shown in Figure 1, where the carrier is still tracked using the conventional phase lock loop, while the code is tracked in the vector mode.

As shown in Figure 1, in each channel, intermediate frequency (IF) signals are first multiplied with the locally generated carrier replica in both in-phase and quadrature arms. Correlation is then performed between the code replicas and the received ones. Afterwards, correlation results are integrated and dumped. The output of these integrations is used as the input to the carrier/code loop discriminator to find the phase error of the local carrier and code replicas. In each carrier loop, the carrier discriminator output is filtered and fed back to the carrier NCO. For the code tracking loop, code discriminator outputs of all channels are forwarded to the navigation processor. In this paper, an EKF is used. The output of the carrier loop filter, i.e., Doppler shift frequency information, is also fed into the EKF to help estimator user velocity and user clock drift.

The EKF estimates the navigation solution based on its system propagation and the measurements, which will be described in detail later. After obtaining the navigation solution, the pseudorange and its rate and the line-of-sight (LOS) vector between the receiver and the satellites are predicted using the satellite ephemeris data. Finally, the predicted pseudo-ranges are used to control the code NCO and fed back to each channel.

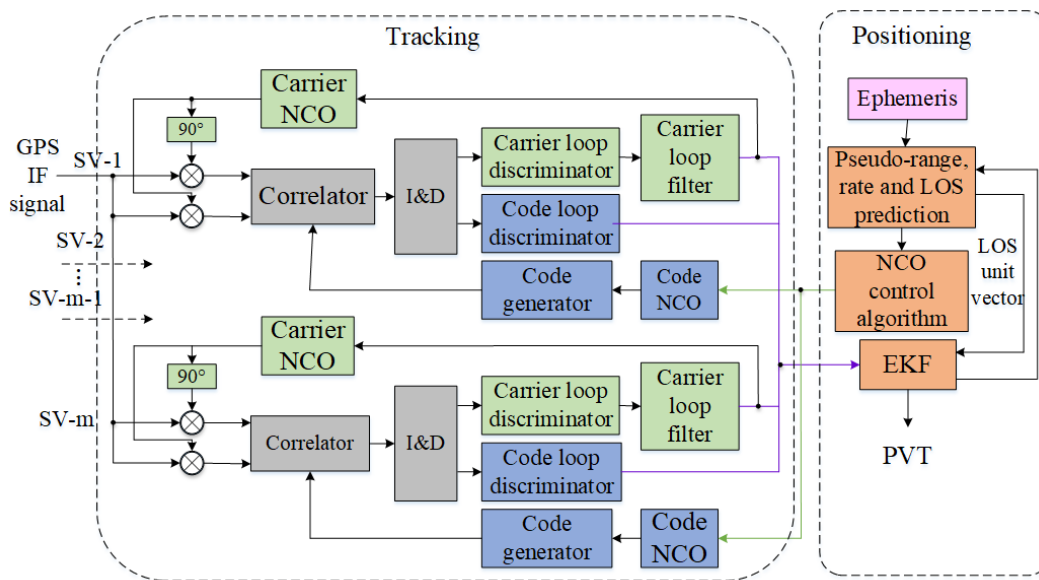


Figure 1: Architecture of vector tracking-based GPS receiver.

Design of EKF

An error state vector-based EKF is used as the navigation solver in this paper, which is expressed as follows

$$\delta \mathbf{x} = [\delta \mathbf{p}, \delta \mathbf{v}, \delta b, \delta d]^T \quad (1)$$

where $\delta \mathbf{p} = [\delta p_x, \delta p_y, \delta p_z]$ and $\delta \mathbf{v} = [\delta v_x, \delta v_y, \delta v_z]$ are 3-dimensional (3D) user position and velocity errors in Earth-centered Earth-fixed (ECEF) coordinate system, respectively; δb and δd are user clock bias and drift in unit of meter and meter per second respectively. The superscript T denotes the transpose of a matrix. The system propagation at epoch k can be given by

$$\delta \mathbf{x}_{k|k-1} = \Phi \delta \mathbf{x}_{k-1} + \mathbf{w}_{k-1} \quad (2)$$

where \mathbf{w}_k is the system noise vector, Φ is the state transition matrix. Let τ be the EKF update interval, then Φ is calculated using the following formulas

$$\Phi = \begin{bmatrix} \mathbf{I}_{3 \times 3} & \tau \mathbf{I}_{3 \times 3} & \mathbf{0}_{3 \times 2} \\ \mathbf{0}_{3 \times 3} & \mathbf{I}_{3 \times 3} & \mathbf{0}_{3 \times 2} \\ \mathbf{0}_{2 \times 3} & \mathbf{0}_{2 \times 3} & \mathbf{K} \end{bmatrix}_{8 \times 8} \quad (3)$$

$$\mathbf{K} = \begin{bmatrix} 1 & \tau \\ 0 & 1 \end{bmatrix} \quad (4)$$

The measurements comprise the pseudorange error, $\delta\rho_k^j$, and the pseudorange rate error, $\delta\dot{\rho}_k^j$, which are derived from the code and carrier tracking loops, respectively, as

$$\delta\rho_k^j = \delta\tau_k^j \cdot c / f_{CA} \quad (5)$$

$$\delta\dot{\rho}_k^j = f_{d,k}^j \cdot c / f_{L1} - (\mathbf{v}_k - \mathbf{v}_k^j) \cdot \mathbf{I}_k^j - \delta d_k \quad (6)$$

where $\delta\tau_k^j$ is the code discriminator output in chips; f_{CA} is the code chipping rate (1.023 MHz for GPS L1 C/A); c is the speed of light; $f_{d,k}^j$ is the Doppler shift frequency in Hz; f_{L1} is the carrier frequency (1575.42 MHz for GPS L1); \mathbf{v}_k and \mathbf{v}_k^j are the velocity vectors of the receiver and satellite j , respectively; $\mathbf{I}_k^j = [l_{x,k}^j \ l_{y,k}^j \ l_{z,k}^j]$ is the LOS unit vector from the receiver to satellite j ; δd_k is the estimated receiver clock drift. The measurement equation is expressed as

$$\delta\mathbf{z}_k = \mathbf{H}_k \cdot \delta\mathbf{x}_{k-1} + \mathbf{v}_k \quad (7)$$

where \mathbf{H}_k is the measurement matrix, calculated by

$$\mathbf{H}_k = \begin{bmatrix} -l_{x,k}^1 & -l_{y,k}^1 & -l_{z,k}^1 & 0 & 0 & 0 & 1 & 0 \\ -l_{x,k}^2 & -l_{y,k}^2 & -l_{z,k}^2 & 0 & 0 & 0 & 1 & 0 \\ \vdots & \vdots \\ -l_{x,k}^m & -l_{y,k}^m & -l_{z,k}^m & 0 & 0 & 0 & 1 & 0 \\ 0 & 0 & 0 & -l_{x,k}^1 & -l_{y,k}^1 & -l_{z,k}^1 & 0 & 1 \\ 0 & 0 & 0 & -l_{x,k}^2 & -l_{y,k}^2 & -l_{z,k}^2 & 0 & 1 \\ \vdots & \vdots \\ 0 & 0 & 0 & -l_{x,k}^m & -l_{y,k}^m & -l_{z,k}^m & 0 & 1 \end{bmatrix}_{2m \times 8} \quad (8)$$

where \mathbf{v}_k is the measurement noise vector, m is the number of satellites involving positioning.

The EKF process noise should be determined by the receiver dynamics and user clock noise characteristics. The measurement noise covariance matrix is calculated adaptively using the measurement innovation. With the navigation solution, code frequency for each channel is predicted using the following equation

$$f_{code,k}^j = f_{CA} \left[1 - \frac{\hat{\rho}_k^j - \hat{\rho}_{k-1}^j}{c \cdot T_0} \right] \quad (9)$$

$$\hat{\rho}_k^j = \|\mathbf{p}_k - \mathbf{p}_k^j\| + \delta\hat{\rho}_{sv,c}^j + \delta\hat{\rho}_I^j + \delta\hat{\rho}_T^j - \delta b_k \quad (10)$$

where $\hat{\rho}_k^j$ and $\hat{\rho}_{k-1}^j$ are the predicted pseudorange at epoch k and the estimated pseudorange at epoch $k-1$. \mathbf{p}_k and \mathbf{p}_k^j are the satellite position and the predicted receiver position at epoch k , respectively. $\delta\hat{\rho}_{sv,c}^j$, $\delta\hat{\rho}_I^j$ and $\delta\hat{\rho}_T^j$ are pseudorange error corrections due to satellite clock error, ionospheric and tropospheric delay, respectively.

NLOS RECEPTION DETECTION AND COMPENSATION ALGORITHM

The proposed NLOS reception detection and correction algorithm is shown in Figure 2. GPS IF data is first processed in a conventional tracking-based software receiver, which outputs the satellites ephemeris and the user position. Vector tracking then begins with this information. In this paper, multiple correlators are implemented to detect the NLOS reception, and to extract the NLOS delay. The code discriminator is a noncoherent early-minus-late envelope discriminator with one chip spacing.

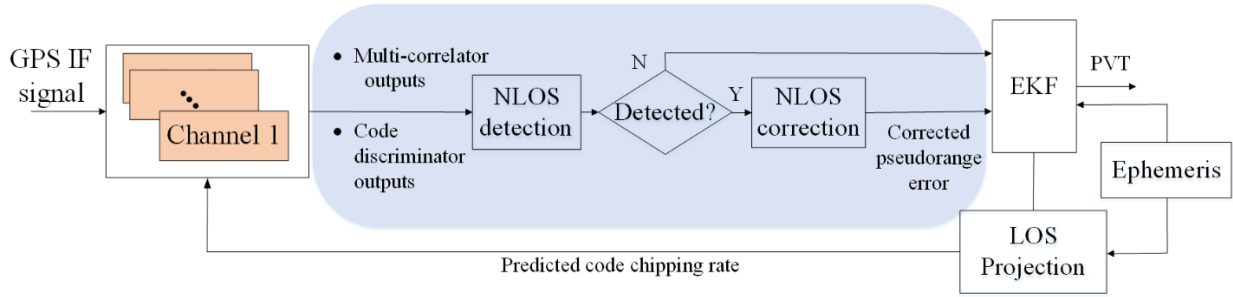


Figure 2: NLOS reception detection and correction algorithm.

Multi-correlator and code discriminator outputs are used as NLOS detection features. In vector tracking loops, code frequency for each satellite is found using both the navigation solution and the prediction of the user dynamic model. Therefore, when NLOS reception occurs, the code replica in the corresponding channel will be aligned with the predicted direct signal instead of the NLOS signal, provided that a good navigation solution is obtained using measurements from other NLOS-free channels. The code phase difference between the code replica and the code in NLOS receptions will manifest itself as the code tracking error, i.e., the code discriminator outputs. Besides, the NLOS reception delay can also be extracted from the multiple correlator outputs.

Once detected, the NLOS reception is generally excluded from the measurements. In urban areas, however, satellite availability is also a critical issue due to severe signal blockages. The exclusion of NLOS signals would lead to degraded satellite availability. In this paper, the multi-correlator in vector tracking could find the delay of the NLOS reception. Thus, it is corrected and exploited in positioning. Detailly, the pseudorange error measurement of the EKF is corrected by

$$\delta\rho_c^j = (\delta\tau^j + \tau_{corr}) \cdot \frac{c}{f_{CA}} \quad (11)$$

where τ_{corr} is the NLOS correction calculated as the mean of 50 consecutive code discriminator outputs. The corrected pseudorange error measurement is used as part of the measurements. With this, the NLOS reception is exploited, which could also improve positioning accuracy instead of contaminating it.

TEST AND RESULTS

To evaluate the NLOS detection and correction performance of the proposed method, a field test was conducted. The test setup and results are described in detail as follows.

Test Environment and Setup

Raw GPS data was collected in an urban area, as shown in Figures 3(a) and 3(b). The pedestrian carrying a NovAtel GPS 702-GG antenna kept static at Point 1 for about 40 seconds before walking towards east to Point 2. The walking trajectory is shown in Figure 3(a). The pedestrian returned to Point 1 along the same trajectory a few seconds later. The walking velocity is about 1 m/s. It is interesting to note that the building on one side of the street is much higher than that on the other side. In particular, one of the tall buildings in the right side is covered by very flat glass, which is a strong reflector to satellite signals. This environment is very common in urban areas, and it easily allows the occurrence of NLOS reception. The data collection equipment includes a NovAtel 702-GG active antenna, a Nottingham Scientific Ltd. (NSL) Stereo front-end with a bandwidth of 2 MHz, and a Dell laptop for data storage, as shown in Figure 3(c). In this paper, 25 correlators with a spacing of 0.05 chip are implemented. The loop prediction integration time is 1 ms. Measurements that shown in Equations (5) and (6) are averaged over 20 ms, resulting in a 20 ms EKF update interval.

The Skymasks (Skyplot with building boundary information) at Point 1 and Point 2 are presented in Figure 4. At Point 1, five satellites are visible according to the Skymask, and all satellites are acquired and tracked successfully by the software receiver. At Point 2, however, PRNs 22 and 31 are blocked by the building on the north side. It should be noted that Skymask can only determine

the satellite visibility but cannot tell which satellite would have a multipath signal. Details of the tests and results are described as follows.

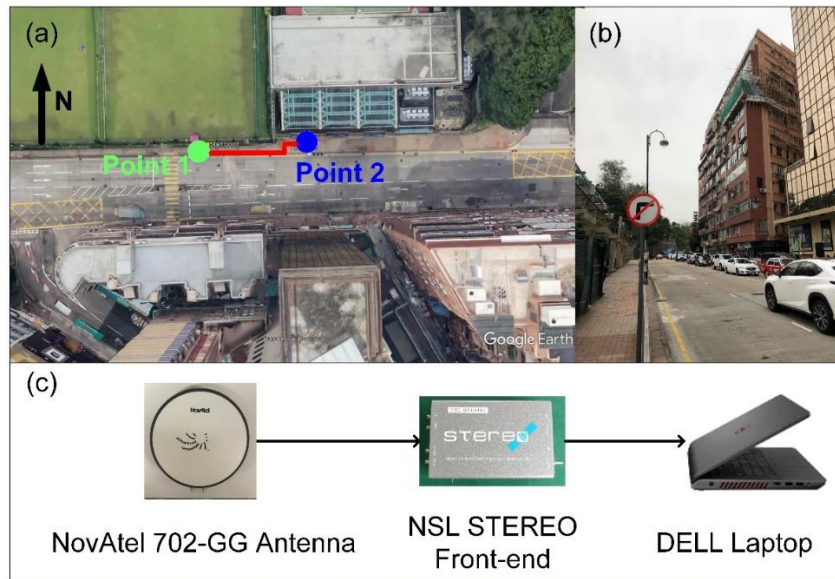


Figure 3: Test environment and setup. (a) Walking trajectory in Google Earth; (b) Environment on both street sides; (c) GPS Raw data collecting equipment.

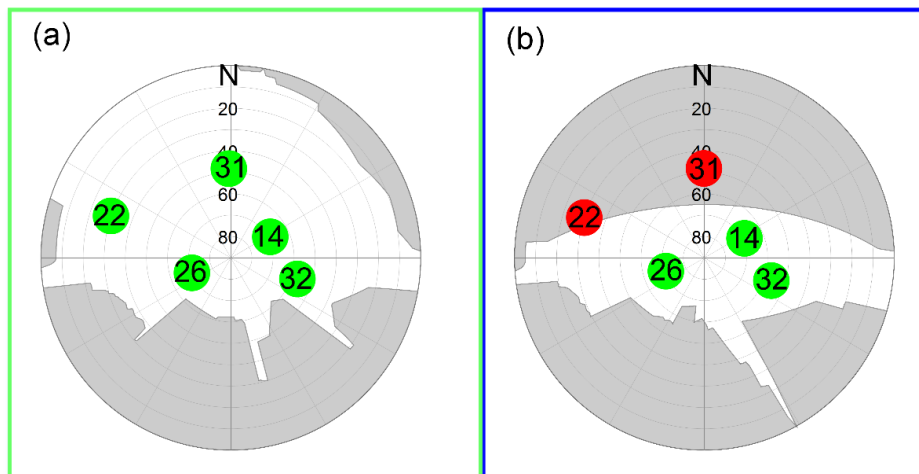


Figure 4: Skymask. (a) Point 1; (b) Point 2.

Test Results

Since the user moves towards east, the east-direction velocity helps to determine the time at which the pedestrian is static or walking, as well as the location. Figure 5 shows the user east-direction velocity and code discriminator output of PRN 31 during the whole test period. It can be seen that CT keeps tracking the incoming signal stably during the whole test. A slightly increased code tracking error during the period of 3400~3600 epochs indicates the degraded signal quality, which also means the signal of PRN 31 is still received by the antenna. This can also be confirmed by the correlation value in the prompt channel, as shown in Figure 6 where navigation bit stream can clearly be seen when the user is at Point 2, although having a lower magnitude than at Point 1. Compared with CT, VT shows a relatively unstable code discriminator output. The periodic oscillation during the static stage indicates the

existence of multipath reception, while the negative value during in the period of 3400~3600 epochs reported a potential reception of NLOS signal from PRN 31, which will be further verified in the following results.

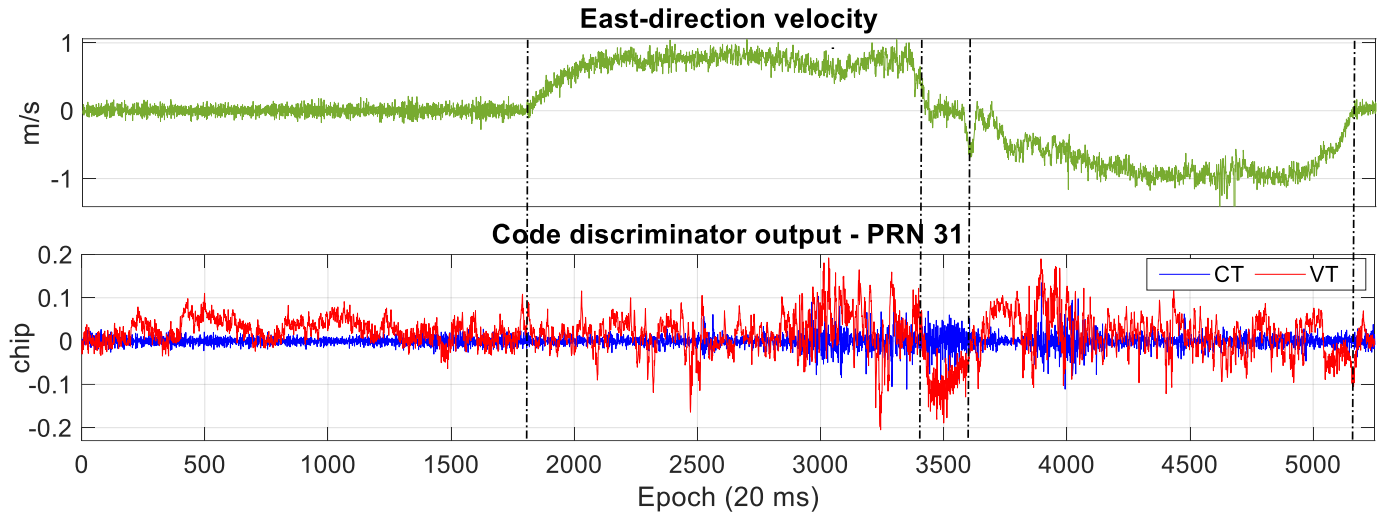


Figure 5: East-direction velocity and code discriminator output of PRN 31 during the test.

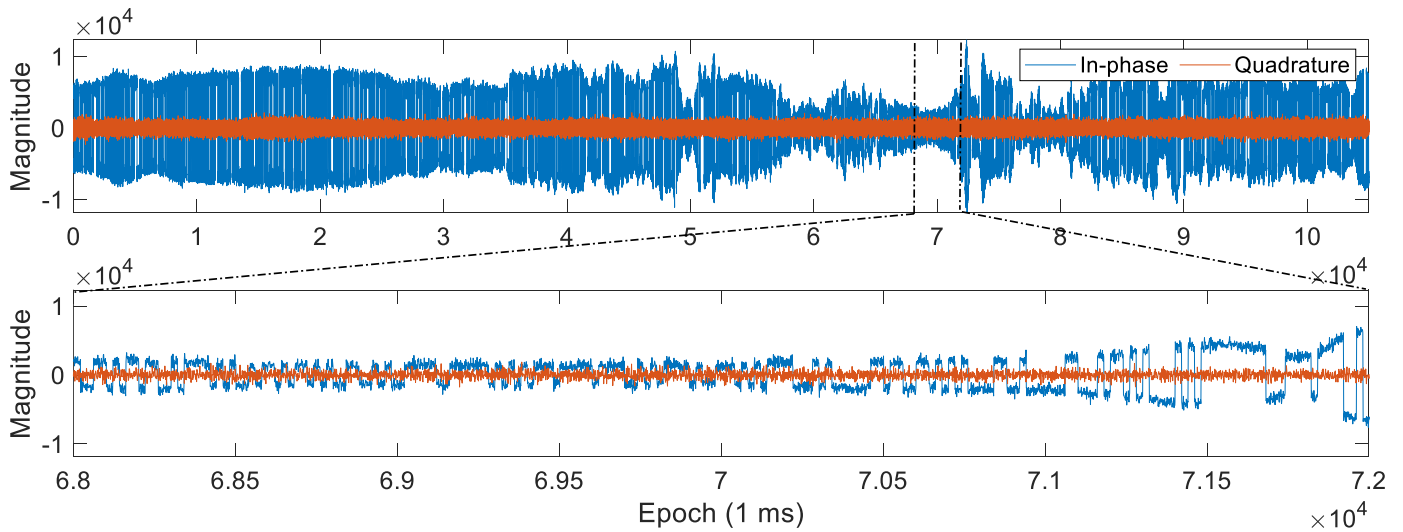


Figure 6: In-phase prompt correlation value at Point 2.

Figure 7 is the multiple correlator outputs of conventional tracking and vector tracking, respectively, at epoch 69000 ms. It is observed that the maximum correlation values are distributed around zero-time delay in conventional tracking loops, which means the local replica in the prompt channel in conventional tracking loops is aligned with the incoming NLOS signal. Therefore, the conventional tracking cannot distinguish the NLOS reception from the incoming signals. In another word, the NLOS reception would be regarded as a direct signal in conventional tracking loops, which would introduce an error into pseudorange measurements. In vector tracking, however, a positive offset of the maximum correlation values is reported. This offset implies that the incoming signal is aligned with one of the late channels in the multiple vector tracking loops. It is known that the NLOS reception is always later than the corresponding direct signal. Thus, the positive offset of the maximum correlation values in vector tracking loops is a good indicator of NLOS reception.

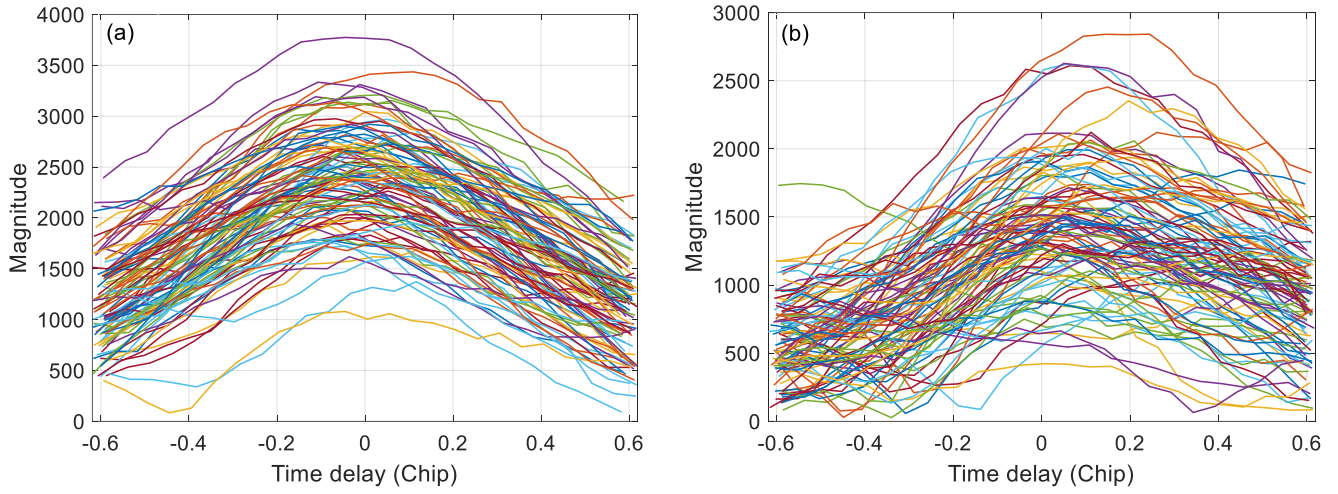


Figure 7: Multiple correlator outputs (overlapping for 100 ms). (a) CT; (b) VT

To quantitatively verify the NLOS detection performance of vector tracking, the variance and mean of the maximum correlation value are extracted as two features for identifying NLOS reception. Figure 8 shows these two features during the NLOS reception period for both conventional and vector tracking loops. For both features, VT has a higher value than CT. This phenomenon can be explained that the code phase difference between the local code replica and the incoming code can be detected in vector tracking due to that the code frequency is predicted based on the navigation solution, while in conventional tracking, the code frequency is adjusted using the code discriminator output.

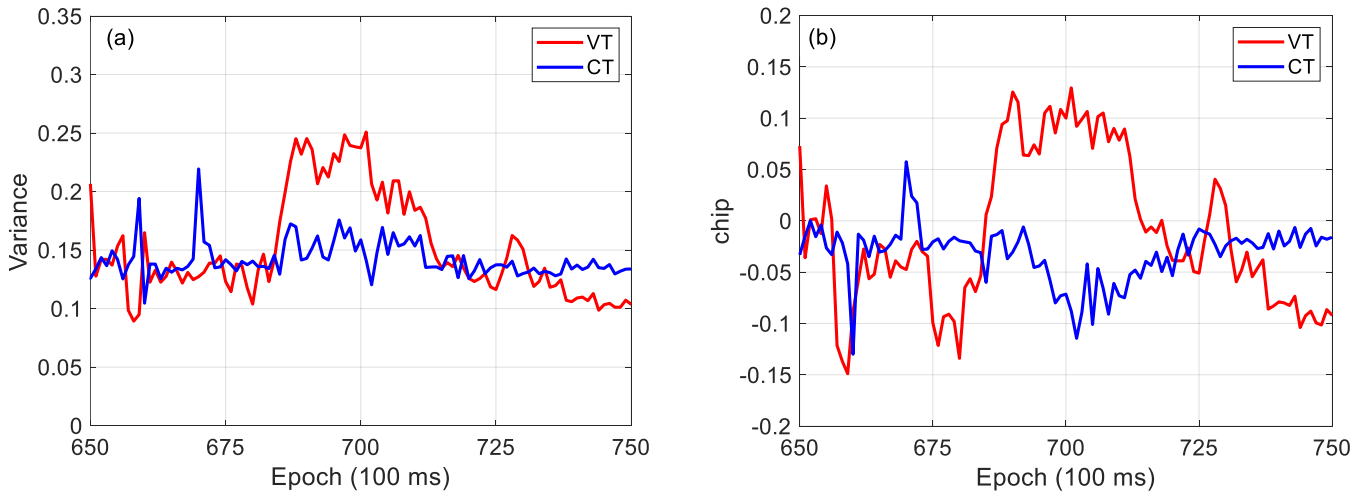


Figure 8: NLOS features extracted from multiple correlator outputs. (a) Variance of the maximum correlation values; (b) Mean of the maximum correlation values.

Once detected, the NLOS code delay in meters, i.e., the NLOS-caused pseudorange measurement error, is corrected according to the multiple correlator outputs. Figure 9(a) shows the detected NLOS code delay in meters. In [1], the NLOS pseudorange delay, γ , is modeled as:

$$\gamma = \alpha \sec \theta_{ele} (1 + \cos 2\theta_{ele}) \quad (12)$$

where α is the distance between the receiver and building that reflects the signal; θ_{ele} is the satellite elevation angle. As shown in Figure 9 (b), α is 20 meters in this test. The elevation angle of PRN 31 is 48.2 degree. Therefore, the NLOS code delay in meters is about 26.8 meters, which is consistent with the detected NLOS delay.

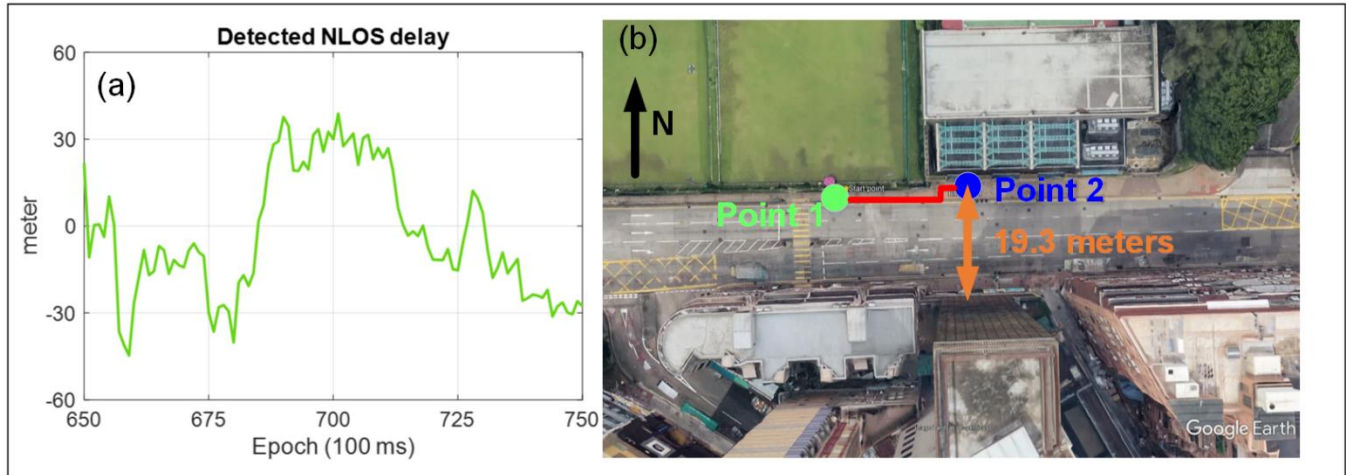


Figure 9: NLOS delay detection. (a) Detected NLOS delay: (b) Street width.

Figure 10 shows the horizontal positioning error of both conventional tracking and vector tracking with NLOS delay correction. As is shown, during the whole test period, VT outperforms CT. During the walking stages, the positioning error increases for CT, while for VT, a good position is still obtained. In particular, during the period of 3400~3600 epochs when NLOS reception occurs, the performance of CT decreases dramatically, while with NLOS detection and correction, VT still reports a high accuracy on positioning. Positioning errors in different periods during the test is listed in detail in Table 1.

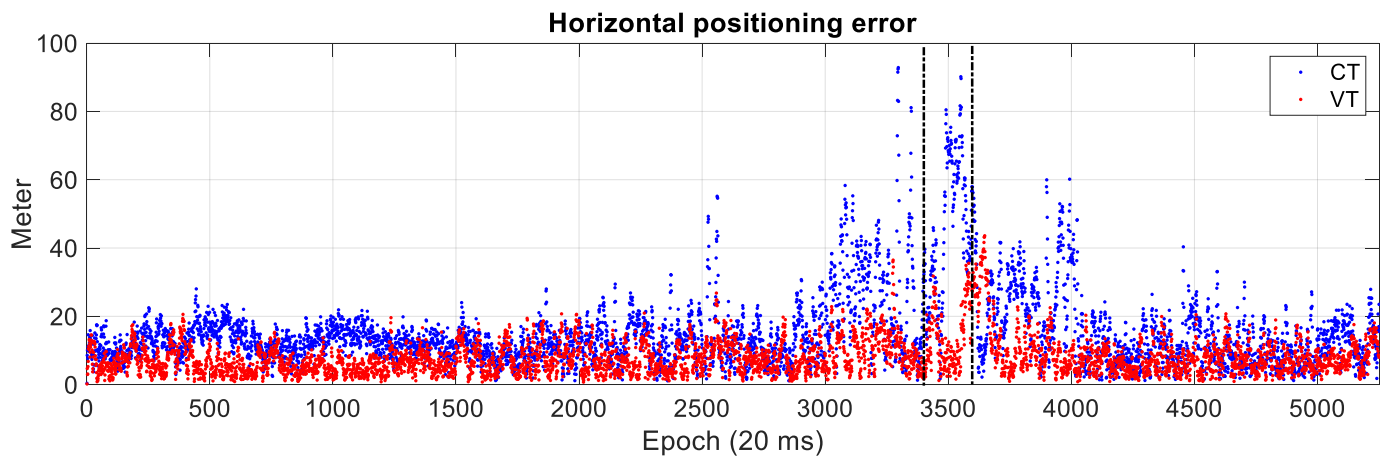


Figure 10: Horizontal positioning error.

Table 1: Horizontal positioning error in different periods during the test (meters)

Epochs	1~1800	1800~3400	3400~3600	3600~5200
VT	6.43	8.39	13.64	8.47
CT	12.14	16.22	45.41	14.67

As shown in Figure 4(b), PRN 22 is also invisible at Point 2. However, as shown in Figure 11, PRN 22 is not predicted to be an NLOS satellite. Notice that PRN 22 is near the building boundary, which probably falls within the diffraction region [10], i.e., the signal is likely to be diffracted.

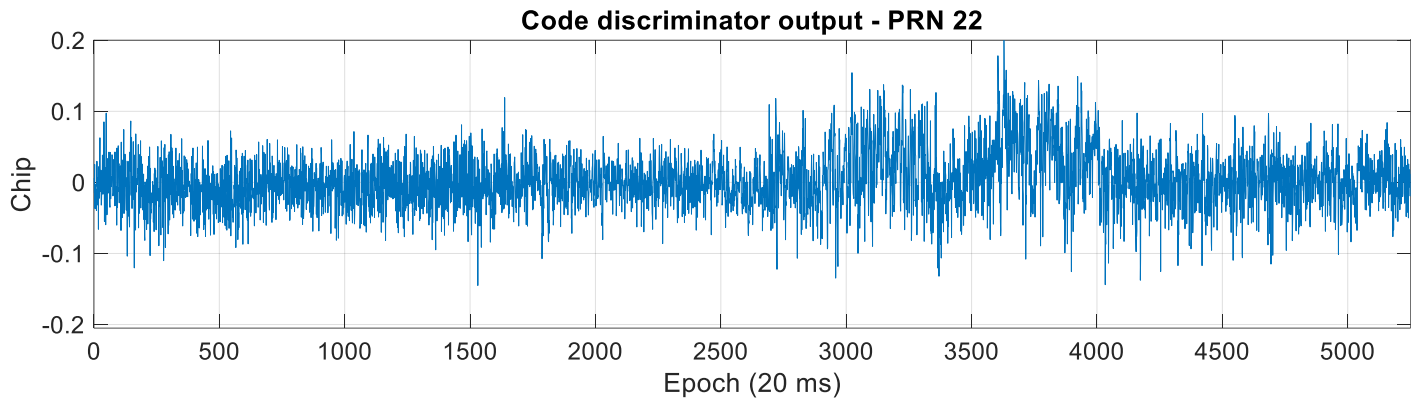


Figure 11: Code discriminator output of PRN 22.

CONCLUSIONS

This paper proposes a multiple correlator-based NLOS detection and compensation method in a vector tracking-based GPS software receiver. The effectiveness of this method is verified by real NLOS receptions. Unlike conventional tracking, vector tracking predicts the code frequency based on the navigation solution, instead of the code discriminator output. Therefore, the local code replica in the prompt channel is not aligned with the incoming code. By monitoring multi-correlator or code discriminator outputs, features, e.g., the variance and mean of the maximum correlation values are extracted for detecting NLOS reception. In addition, multiple correlators with a small spacing help to find the NLOS code delay, which is further compensated to do positioning. Compared with conventional, vector tracking with NLOS detection and compensation shows a greatly improved positioning performance.

A natural progression of this work is to explore the potential of multipath signal detection and compensation using multi-correlator-based vector tracking loops.

ACKNOWLEDGMENTS

The authors acknowledge the support of Hong Kong PolyU startup fund on the project 1-ZVKZ, "Navigation for Autonomous Driving Vehicle using Sensor Integration".

REFERENCES

1. Hsu, L.-T., "Analysis and modeling GPS NLOS effect in highly urbanized area," *GPS Solutions*, Vol. 22, No. 1, 2018, pp. 7.
2. Zhdanov, A., Zhodzishsky, M., Veitsel, V., and Ashjaee, J., "Evolution of multipath error reduction with signal processing," *GPS Solutions*, Vol. 5, No. 3, January 2002, pp. 19-28.
3. McGraw, G. A., Young, R. S. Y., Reichenauer, K., Stevens J., and Ventrone, F., "GPS multipath mitigation assessment of digital beam forming antenna technology in a JPALS dual frequency smoothing architecture," *Proceedings of the 2004 National Technical Meeting of The Institute of Navigation, San Diego, CA, January 2004*, pp. 561-572.
4. Jiang Z., and Groves, P. D., "NLOS GPS signal detection using a dual-polarisation antenna," *GPS Solutions*, Vol. 18, No. 1, January 2014, pp. 15-26.
5. Suzuki T., and Kubo, N., "N-LOS GNSS signal detection using fish-eye camera for vehicle navigation in urban environments," *Proceedings of the 27th International Technical Meeting of The Satellite Division of the Institute of Navigation (ION GNSS+ 2014), Tampa, Florida, September 2014*, pp. 1897-1906.

- 6 Sanchez, J. S., Gerhmann, A., Thevenon, P., Brocard, P., Afia, A. B., and Julien, O., "Use of a FishEye camera for GNSS NLOS exclusion and characterization in urban environments," *Proceedings of the 2016 International Technical Meeting of The Institute of Navigation, Monterey, California, January 2016*, pp. 283-292.
- 7 Wen, W., Zhang, G., and Hsu, L.-T., "Correcting GNSS NLOS by 3D LiDAR and building height," *Proceedings of the 31st International Technical Meeting of The Satellite Division of the Institute of Navigation (ION GNSS+ 2018), Miami, Florida, September 2018*, pp. 3156-3168.
- 8 Groves, P. D., "It's time for 3D mapping-aided GNSS," *Inside GNSS*, September 2016, pp. 50-56.
- 9 Groves, P. D., "Shadow matching: a new GNSS positioning technique for urban canyons," *The Journal of Navigation*, Vol. 64, No. 3, Jul 2011, pp. 417-430.
- 10 Wang L., Groves, P. D., and Ziebart, M. K., "GNSS shadow matching: improving urban positioning accuracy using a 3D city model with optimized visibility scoring scheme," *NAVIGATION*, Vol. 60, No. 3, 2013, pp. 195-207.
- 11 Wang, L., Groves, P. D., and Ziebart, M. K., "Smartphone shadow matching fo better cross-street GNSS positioning in urban environments," *Journal of Navigation*, Vol. 68, No. 3, 2015, pp. 411-433.
- 12 Hsu, L.-T., Gu, Y., and Kamijo, S., "NLOS Correction/Exclusion for GNSS Measurement Using RAIM and City Building Models," *Sensors*, Vol. 15, No. 7, 2015, pp. 17329-17349.
- 13 Groves, P. D., Jiang, Z., Wang, L., and Ziebart, M. K., "Intelligent urban positioning using multi-constellation GNSS with 3D mapping and NLOS signal detection," *Proceedings of the 25th International Technical Meeting of The Satellite Division of the Institute of Navigation (ION GNSS 2012), Nashville, TN, September 2012*, pp. 458-472.
- 14 Jiang, Z., and Groves, P. D., "GNSS NLOS and multipath error mitigation using advanced multi-constellation consistency checking with height aiding," *Proceedings of the 25th International Technical Meeting of The Satellite Division of the Institute of Navigation (ION GNSS 2012), Nashville, TN, September 2012*, pp. 79-88.
- 15 Hsu, L.-T., Tokura, H., Kubo, N., Gu, Y., and Kamijo, S., "Multiple faulty GNSS measurement exclusion based on consistency check in urban canyons," *IEEE Sensors Journal*, Vol. 17, No. 6, 2017, pp. 1909-1917.
- 16 Suzuki, T., Nakano, Y., and Amano, Y., "NLOS multipath detection by using machine learning in urban environments," *Proceedings of the 30th International Technical Meeting of The Satellite Division of the Institute of Navigation (ION GNSS+ 2017), Portland, Oregon, September 2017*, pp. 3958-3967.
- 17 Hsu, L.-T., Groves, P. D., and Jan, S. S., "Assessment of the multipath mitigation effect of vector tracking in an urban environment," *Proceedings of the ION 2013 Pacific PNT Meeting, Honolulu, Hawaii, April 2013*, pp. 498-509.
- 18 Hsu, L.-T., Jan, S. S., Groves, P. D., and Kubo, N., "Multipath mitigation and NLOS detection using vector tracking in urban environments," *GPS Solutions*, Vol. 19, No. 2, April 2015, pp. 249-262.
- 19 Pany, T., and Eissfeller, B., "Use of a vector delay lock loop receiver for GNSS signal power analysis in bad signal conditions," *Proceedings of 2006 IEEE/ION Position, Location, And Navigation Symposium*, Coronado, CA, USA, 2006, pp. 893-903.
- 20 Lashley, M., Bevely, D. M., and Hung, J. Y., "Performance analysis of vector tracking algorithms for weak GPS signals in high dynamics," *IEEE Journal of Selected Topics in Signal Processing*, Vol. 3, No. 4, 2009, pp. 661-673.
- 21 Xu, B. and Hsu, L.-T., "An open source Matlab code on GPS vector tracking based on software-defined receiver," *GPS Solutions*, 23:46, DOI: 10.1007/s10291-019-0839-x, 2019.